Earthq Eng & Eng Vib (2021) 20: 63-78 **DOI**: https://doi.org/10.1007/s11803-021-2005-z

Topographic effects observed at Amatrice hill during the 2016–2017 Central Italy seismic sequence

Gerardo Grelle[1†], Laura Bonito[2‡], Maresca Rosalba[2§], Silvia Iacurto[1‡], Claudia Madiai[3*], Paola Revellino[2*] and Giuseppe Sappa[1*]

1. *Department of Civil, Building and Environmental Engineering, Sapienza University of Rome, Italy*
2. *Department of Sciences and Technologies, University of Sannio, Italy*
3. *Department of Civil and Environmental Engineering, University of Florence, Italy*

Abstract: The estimate of seismic site effects by experimental approaches is based on different assumptions aimed at simplifying the complex actual site conditions and related uncertainties. However, the reliability of the results can increase if the experimental data is focused on quite strong seismic sequences and the on-site acquisition of a large number of signals is deemed strategic for the assessment of the expected phenomena. Based on these considerations, the ground motion at the Red Zone sector of Amatrice hill, violently struck by the 2016–2017 Central Italy seismic sequence, was analyzed via an observational approach. A large set of weak motions (moment magnitude M_w 2.5–3.9) was analyzed in this study by means of standard (SSR) and horizontal to vertical (HVSR) spectral ratio techniques. The results from the experimental analysis of the site effects by using weak motion and noise signals show a significant amplification at the top of Amatrice hill with a remarkable polarization of the motion and changes in spectral shapes according to the topographic setting of the relief.

Keywords: topographic effects; standard spectra ratio (SSR); horizontal and vertical spectral ratio (HVSR); directional effects

1 Introduction

1.1 Background

Damage observed during numerous recent and past earthquakes has shown that seismic ground motion strongly depends on the geo-lithological and geomorphological features of the site, soil dynamic behavior, and their combination. Thus, at several sites, seismic shaking can considerably exceed the average amplitude of the shaking affecting the surrounding areas (Bakir *et al*., 2002; Dolce *et al*., 2003, among others). The evaluation of seismic site effects may be particularly difficult if topography and/or buried structures interact with the waveforms (Hough *et al*., 2010; Hartzell *et al*., 2014; Madiai *et al*., 2016, 2017; Facciorusso *et al*., 2016; Ba *et al*., 2017), producing both changes in the vibration direction and in seismic ray path, and generation of surface waves (Sanchez-Sesma *et al*., 1989; Kawase and Aki, 1990; Kawase, 1996; Rovelli *et al*., 2001; Narajan and Singh, 2006; Maufroy *et al*., 2017; Wirth *et al*., 2018; Jahromi and Karkhaneh, 2019).

Seismic site effects (SSE) have been historically studied by means of the analysis of seismic records, by numerical simulation approaches, or via a combination of the two approaches (for a complete review of the methods, see Sanchez-Sesma *et al*., 2010). Since the different theoretical approaches are based on different models and simplifying assumptions, their performance needs to be related to the complexity of the site conditions. The epistemic uncertainties that affect SSE evaluation mainly concern the site modelling stemming from geological and geophysical investigations, the geotechnical parametrization, as well as the computational modelling used in simulations. The techniques to estimate seismic site effects by using experimental data generally consider spectral ratios with respect to one or more reference stations, such as SSR (standard spectral ratio) (Borcherdt, 1970) and MSR (median spectral ratio) techniques (Wood and Cox, 2016) and/or single stations measurements, such as the HVSR (horizontal-to-vertical spectral ratio) approach (Mucciarelli and Gallipoli, 2001; Haghshenas *et al*., 2008; Lunedei and Malischewsky, 2015; Maresca *et al*., 2018). In particular, the SSR method considers the spectral amplification by performing the ratio of the signal recorded at the stations located on relief (ridge and slopes) and one station at the base of the relief. This

Correspondence to: Gerardo Grelle, Department of Civil, Building and Environmental Engineering, Sapienza University of Rome, Via Eudossia 18- 00184 Roma, Italy
Tel: +39 06 44585006
E-mail: gerardo.grelle@uniroma1.it
[†]Assistant Professor; [‡]PhD; [§]Lecture; [*]Professor
Received November 10, 2019; **Accepted** August 12, 2020

station is sited in a valley zone, where the ground motion does not suffer amplifications/de-amplifications due to geological (outcropping rock) and topographic (flat surface) features of the site. In contrast, the HVSR is the spectral ratio from horizontal and vertical spectral components assuming that the signal is composed of surface waves (for stationary microtremor) and that the ellipticity of the signals does not change the amplitude of the vertical component when changing the site impendence contrast due to soil stiffnesses variation in a flat site. The most general simplification assumed by the HVSR method is that site amplification/de-amplification does not affect the vertical component of the ground motion. The SSR approach is based on the assumption that seismic site effects at the reference station are negligible. By introducing the virtual reference station as a spectral median of all stations, the MSR aims to exclude the simplification that comes from considering only one reference station. However, in the MSR method, it can be difficult to quantify the influence of the signals recorded at the top of the hill when a low number of stations are used. In many cases, it can be difficult to identify a single representative station where the influence of both stratigraphic and topographic effects is negligible. For this reason, some techniques, as the MSR approach, try to minimize the above-mentioned effects using a reference virtual station obtained as the spectral median of all the others. However, this latter approach requires a significant number of stations distributed on all the different sectors of the area under study. Experimental techniques have the undeniable advantage that they do not require a thorough knowledge of the geo-lithological and geomorphological features of the site. In addition, thanks to the orthogonal orientation of the sensors, they permit an analysis of the possible directionality of the amplification. Numerous experimental studies have revealed that the prevailing spectral vibration provides an appropriate marker for detecting topographic effects and that the highest amplification of seismic vibrations in elongated reliefs occur in the direction of the transversal axis (Buech *et al*., 2010; Sohrabi Bidar *et al*., 2009; Saeed and Sama, 2019; Hakima *et al.*, 2019). However, the main shortcoming of experimental approaches concerns the use of seismic noise or very low-seismicity that entails an inappropriate evaluation of the site response in case of high cyclic shear strain levels that induce nonlinear soil behavior effects. In addition, the results obtained from these approaches are only locally valid because they investigate the combined effect rather than the causes that promote such an effect. Consequently, the area investigated by using these approaches is generally defined by the number and the geometric arrangement of the recording station network, and to a lesser extent by the complexity of the site conditions. In some cases, the analysis of a large data set of events (Di Alessandro *et al*., 2012; Gallipoli *et al*., 2014), or noise recordings (Mucciarelli *et al*., 2003; Haghshenas *et al*., 2008; Bonnefoy-Claudet *et al*., 2009; Cara *et al*., 2010), provided a statistical validation of the experimental estimates. However, although these techniques suffer from the previously mentioned simplification/shortcoming, they have the advantage of using actual seismic records.

1.2 Case study framework

The experimental analyses, which are the subject of this paper, aim to provide information regarding the role of seismic topographic effects at Amatrice hill. The study is based on significant data from seismic recordings acquired by four stations of a temporary network located at strategic sites (three at the top of Amatrice hill and one at its base) and two stations of the Italian Strong Motion Network (one close to the edge of the hilly promontory and the other at the base of the hill). Specifically, SSR technique on weak-motions and HVSR on weak-motions and noise recordings were used in this study to recognize topographic effects on three different areas at the top of the hill: at the edge of the promontory, at the border of a steep slope, and in the center of the hill. The results from HVSR analyses were used to detect the spectral range of ground motion amplification and were compared with the results from SSR analyses to define an amplification function considering the topographic effects. Specifically, the study focused on a directional analysis of the ground motion amplification detected by both experimental methods, intending to highlight the different site responses in different sectors of the hilly plateau by contextualizing such results also with the global and local geometry of the relief and in comparison with the Apennine chain orientation. In addition, geophysical surveys were carried out with the aim to define the lithological sequence at the top of the hill based on wave propagation velocity profiles. Finally, a study of the topographic effects on strong motion recordings was performed by analyzing the signals recorded at two stations of the Italian Strong Motion Network.

In this framework, note that after the 2016-2017 Central Italy seismic sequence, Amatrice was included in the project "Interventi urgenti in favore delle popolazioni colpite dagli eventi sismici del 2016 (Urgent measures for the populations affected by the 2016 seismic sequence)" that was funded by the Italian Civil Protection Department (DPC) - Special Government Commissioner of the Presidency of Council of Ministers - and coordinated by the "Centro per la Microzonazione Sismica e le sue Applicazioni" to support the reconstruction in 137 municipalities most damaged by the earthquakes. Geological, geotechnical, and geophysical investigations and microzoning studies were carried out within this project in Amatrice′s municipal area; the main results have been summarized in several papers by the Italian scientific community operating in the field of seismic site effects and microzoning (Gaudiosi *et al*., 2019; Pergalani *et al*., 2019; among other).

Thus, the present work benefits from reference elements and additional data from the above-mentioned project that decrease uncertainties and, consequently, strengthen the final hypothesis assumed and the results obtained. In this regard, preliminary studies and investigations on the role of topographic effects on Amatrice hill (Grelle *et al.*, 2018a; Grelle *et al.*, 2020) have substantially been confirmed by recent further studies based on data from geophysical investigations performed by "Istituto Nazionale di Geofisica e Vulcanologia" (National Institute of Geophysics and Vulcanology) team (Milana *et al.*, 2019). In addition, the data produced from this study were also used to support the computational analysis reported in Grelle *et al.*, 2020. In this last reference, the experimental data have been permitted to assume the litho-stratigraphic input model, by means of the HVSR analysis; and to validate the preliminary seismic response in linear shear strain condition at the top hill sites hosting the broad-band permanent stations by means of the SSR analysis.

2 Amatrice area features

Amatrice village is located in a lithologically and topographically complex area that incurred the majority of damage during the recent 2016–2017 seismic sequence of Central Italy (Amatrice-Visso-Norcia), with the greatest loss of human life in the first strong event of August 24th, 2016, moment magnitude M_w = 6.0. The seismic sequence continued with the October 30th event of the same year (M_w = 6.5) and ended with the serial events of February 18th–19th 2017 (M_w = 5.0 and 5.5) (Fig. 1(a)). The most damaged Amatrice zone was the historic center. The extensive and widespread damage over this sector induced the authorities to declare it as a "Red Zone" (an off-limits zone due to the high danger level), as early as the day after the 24th August event.

Amatrice hill is a part of the mountain/hilly Apennine Chain, in the central sector of Central Italy, that developed during the Oligocene-Quaternary times in a NW-SE-trending fold-thrust belt with a thickness that exceeds 40 km (Cavinato and Celles, 1999; Pauselli *et al.*, 2006). It is composed of Meso-Cenozoic limestones/dolostones which are topped by syn- and post-orogenic siliciclastic marine-turbiditic deposits named the Monti della Laga Formation (Messinian - Pliocene). The latter are formed by sandstone with intercalations of marls and siltstones. Conglomerate/puddingstone heteropic deposits are also frequently present. At the top of the sequence, younger (Quaternary) soils consisting of colluviums or old alluvium deposits fill the topographic depressed areas, and cover the gentle slopes and the ridge of the hills (Geological Map of Italy, 1955; Pagliaroli, 2016). Alluvial/debris fans and landslides deposits also belong to these last deposits.

Amatrice village lies on a hilly plateau which is elongated, for approximately 2 kilometres, in a northwest – southeast direction, in agreement with the Apennine chain alignment (Fig. 1(b)). The more prominent sector at the NW edge of the hill is the Red Zone. It is approximately 500–600 meters long, 200–400 meters wide and rises up 50–70 meters high from the valley. In addition, it is bordered by a steep slope (approximately 30°) to the north and to the west, and by a gentler slope (approximately 15°) to the south.

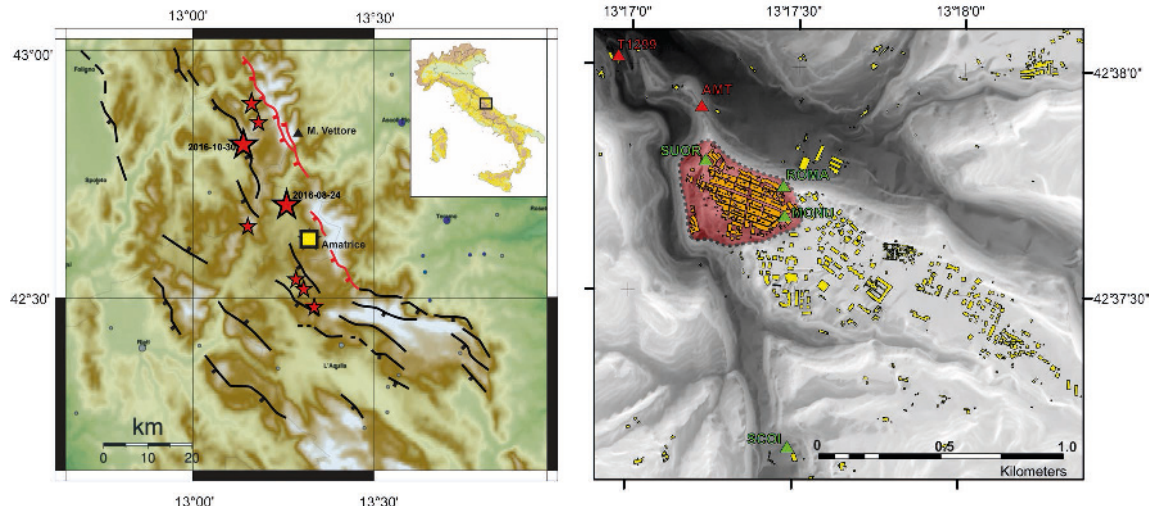

(a) (b)

Fig. 1 (a) Seismotectonic framework of the study area and epicenters of the 2016-2017 events with moment magnitude M_w > 5 (pink stars). The solid black lines indicate the major active faults (Boncio *et al.*, 2004); the red lines represent the recent active fault system (Cheloni *et al.*, 2017). In the time sequence, the M_w of the main shocks were: M1 = 6.0 (24th August 2016); M2=5.5; M3=5.9; M4=6.5 (30th October 2016); M5=5.1; M6=5.5; M7=5.4; M8=5.0. b) Amatrice hill landscape, Red Zone (red polygon) and seismic mobile stations (green triangles) and permanent station of the Italian Seismic Network (red triangles)

2.1 Geo-lithological and geophysical sequence

The geo-lithological units characterizing the subsoil of the Amatrice hill zone are combined to define different sequences (Fig. 2(a)). The hill framework is constituted in sequence by weak siltstone and sandstone on stiff conglomerate and sandstone material. This bedrock outcropping in some parts along the border steep slope and is covered by recent colluvial deposit (Fig. 2(b)) (Grelle *et al*., 2020). The interpretation and correlation of V_s profiles (Fig. 3(a)) together with geological survey information, available geological maps, and borehole stratigraphic logs, permit defining the subsoil sequence that characterizes the Red Zone of Amatrice at the top of the hill, and, in minor detail, the valleys. Figure 3(b) shows the characteristic general stratigraphic sequence of the geo-lithological units in the subsoil model. Shear wave velocity and thickness of each geo-lithological unit vary within the study area. The characteristic stratigraphic sequence includes a basal rock (ML-h), beginning above a depth of 50–60 meters, with an average V_s of 1138 m/s, consisting of sandstone and marly-sandstone/marly-limestone with conglomerate inclusions. This lithological unit may change at the top in a weaker rock (ML-w) characterized by an average V_s of 578 m/s and composed of sandstone and siltstone, and subordinately of very dense sandy material.

Both ML-h and ML-w are members of the "Monti della Laga" units. Soft covering materials follow moving upwards in the sequence and characterize the top of Amatrice hill and the bottom valleys. These soft materials vary within the area in composition and thickness. A layer of an ancient coarse sandy alluvial deposits (AD) extends down to 15–20 meters in depth with an average V_s value of 382 m/s. Near the ground surface, colluvium, and/or anthropogenic deposits (CD), with an average V_s value of 220 m/s, may be found almost everywhere at the top of the succession, and slope debris of similar materials covers the slopes of the plateau with the exception of the steeper zones. In addition, the CD geo-lithological unit is frequently mixed with recent alluvial deposits (SD). These latter, characterized by an average V_s of 293 m/s, consist of depositional filling materials of the valleys and they also fill a topographic depression in the southern-west sector of the hill. The above described sequence covered a large part of the Red Zone and is characterized by linear resonance frequency in the interval of 2–3 Hz.

3 Site response by observational analysis

3.1 Acquired experimental data

Four temporary seismic stations were installed in different sites: SUOR, ROMA and MONU at the top of the hill in the Red Zone and SCOI at the base (Fig. 1(b)). The stations were equipped with broad-band velocity transducers, Trillium compact 120 s (Nanometrics) and 24 bit Centaur digital recorders (Nanometrics) at 100 samples/s (Table 1). Data from two other permanent stations of the Italian Strong Motion Network installed by the national Civil Protection Department (DPC), T1299 and AMT (Fig. 1(b)), was also used. Ambient noise, weak, and strong motion recording data was collected to investigate site effects in the Amatrice area. In particular, results from spectral and directional analyses on weak motion events and noise recordings are reported and discussed below.

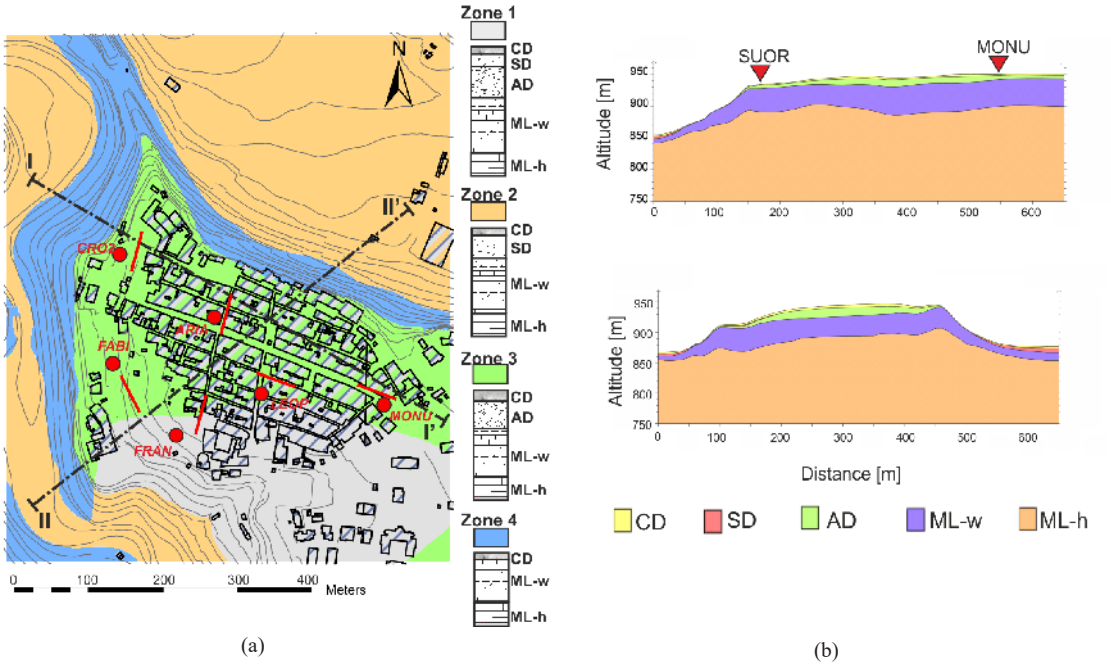

Fig. 2 Extract from Grelle *et al*., 2020: a) map of zones characterizing the stratigraphic sequence; b) transversal and longitudinal cross-section of the Amatrice relief

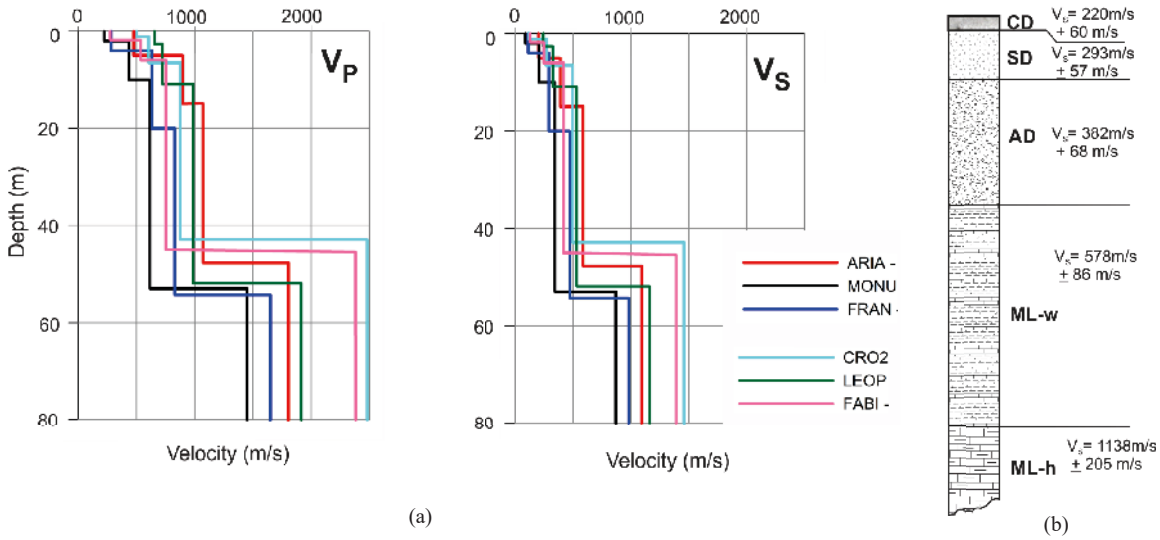

Fig. 3 a) Best-fit V_s and V_p profiles obtained at all the HVSR-MASW sites; b) general stratigraphic sequence of the geo-lithological units

Table 1 Number of seismic weak motion events recorded from January 1st to March 18th (Round 1) and from May 12th to August 10th (Round 2)

Station	Site-source azimuthal direction	Number of seismic events separated for magnitude classes				
		Round	2.5≤*M*<3.0	3≤*M*<3.5	3.5≤*M*≤4.0	Total
T1299	All	1	65	21	4	90
SCOI	All	1	14	3	1	18
SUOR	All	1	61	21	3	85
SUOR	Apennine	1	41	13	0	54
SUOR	Anti-Apennine	1	20	8	3	31
T1299	All	2	30	9	5	44
ROMA	All	2	25	6	4	35
MONU	All	2	27	9	5	41

T1299 permanent station was installed by the DPC in the valley area (approximately 400 m northwest of the Red Zone) after the August 24th event, while AMT is the historical permanent accelerometric strong motion station located in the proximity of the Red Zone (approximately 200 m north) along a crest of a dorsal. It was the only station in Amatrice area that recorded the main August 24th earthquake. AMT weak motion recordings were not used in the analysis, but strong motion data from this station (Table 2) obtained additional quantitative evidence of the topographic directional effects thanks to its location. From each station, seismic data was collected in two different time periods (Round 1 and Round 2) and at different intervals of times, in relation to unfavorable weather conditions and snowfall that prevented the solar power recharging of the instrument batteries (Table 1). The two rounds were necessary because we have only three broadband stations which were insufficient for cover all the zones potentially affect by relevant topographic effects. However, the high number of aftershocks, that were recorded in each round with respect to the T1299 station in the same tectonic regional regime, reasonably assumed that the comparison of the results in terms of spectral amplification in SSR and HVSR are only slightly influenced by using two different periods of acquisition. The longer recording time at the SUOR station provided more seismic waveforms than the other stations; this permitted a robust statistical analysis of the site amplification also with reference to the two main directions (Apennine and anti-Apennine) of the source-station azimuths to be performed and an analysis of the eventual influence of local and regional underground structures on the directionality of the vibration.

All the stations recorded seismic weak-motion signals as well as noise, and both types of signals were used to perform standard spectral ratio (SSR) and horizontal-to-vertical-spectral ratio (HVSR) analyses. With regards to the SSR analysis, between the valley stations T1299 and SCOI, the T1299 station was assumed as a reference station. This assumption is based on the

direct observation of the outcropping bedrock in the near area and on the flat shape of the HVSR curves resulting from the recordings, as well as on the low impedance contrast detected through the MASW surveys that were performed close to this station. In addition, this station was also used as a reference in the study of Milana *et al*., 2019. On the contrary, SCOI station was further away from Amatrice hill, but does not show flat HVSR as expected because of the subsoil lithology at the site where it was installed. All other stations were not taken into consideration as a reference station because they were located at the top of the hill in areas most likely affected by topographic effects.

3.2 Spectral analysis

First, the seismic signals to be processed were manually selected among those of the events with epicenters lesser than 20 km from Amatrice. Then, the selected time series were corrected for the baseline, tapered with a 5% Hanning function, and a bandpass filter from 0.3 to 35 Hz. Fast Fourier transform was applied and raw spectra were smoothed using a Konno and Ohmachi (1998) filter, with a coefficient b=40. Data was statistically analyzed in terms of median, 16th and 84th percentiles. Standard spectral ratios (SSRs) were computed for the NS and EW spectral components at SUOR, ROMA, MONU and SCOI stations, with reference to the corresponding horizontal spectral amplitudes computed at T1299 station.

SSR analyses were performed on the time-windows for the events that had been simultaneously recorded by the target stations (SUOR, MONU, ROMA, and SCOI) and by T1299 station. The results (Fig. 4) highlight a significant amplification at all the target stations compared to T1299, in the frequency range of 1–20 Hz for each component of the ground vibration. Specifically, a marked peak can be observed for all the vertical components (Z) around 10–15 Hz. The median value of the spectral ratio is much greater for the stations on the hill top (SUOR, ROMA, and MONU) than for the SCOI station at the base of the hill. On the other hand, both the horizontal components (NS and EW) show significant amplification median values in a wide range of frequencies: similar trends of average amplitude are observed for the EW component, regardless of recording station, time period recording (Round 1 or Round 2) and site-source azimuth (Apennine or Anti-Apennine), with a pronounced peak at about 10 Hz; on the contrary, the NS component shows different trends of the amplification median curves depending on the different conditions.

The SUOR station, located close to the edge of the hill (Fig. 1(a)), shows two significant amplification peaks (over 5) around 3–3.5 Hz and 9–10 Hz, with a substantial difference between the NS and EW components. For this site, longer recording periods allowed the signals to be analyzed by identifying two different sets since the site-source azimuth distribution was clustered along two preferential alignments: Apennine (similar to orientation of Amatrice promontory) and anti-Apennine. In this regard, the amplification shows a substantial matching in both the horizontal components. Only around 3 Hz and for the NS component, the median value of the amplification for the events with azimuths in the anti-Apennine direction (that is transversal to the hilly promontory) is considerably greater than those calculated for the events with azimuths in the Apennine direction.

The ROMA station, located on the ridge of the northern steep-slope, shows significant amplification, with median peak values in an extensive spectral range (2–10 Hz). A substantial difference in the two horizontal spectral amplification was observed. SSR computed on the NS component shows larger amplification values in all the range of frequencies of 2–10 Hz around the median values of 7. On the other hand, for the EW component, the maximum amplification values (>10) are observed at higher frequencies, around 8–10 Hz; however also at these higher frequencies, the 2 Hz sustained the amplification. The higher peak at 10 Hz, which was observed in the NS component but was not present in the EW component, seems to be the more relevant difference.

The MONU station, located in the central sector of the hill, shows maxima in the SSR curves lower than those observed for the two other stations on the hill top. Significant amplification is observed around 2 Hz

Table 2 List of strong motion events whose epicenters are plotted in Fig. 1(a)

Earthquake ID	Station	M_W	PGA_{NS} (m/s^2)	PGA_{EW} (m/s^2)
M1	AMT	6.0	3.68	8.53
M2	AMT	5.4	0.60	0.89
M3	AMT	5.9	0.59	0.91
M4	AMT	6.5	3.94	5.24
M4	T1299	6.5	4.37	4.45
M5	AMT	5.1	3.56	1.97
M6	AMT	5.5	3.20	3.07
M7	AMT	5.4	1.15	1.56
M8	AMT	5.0	0.49	0.57

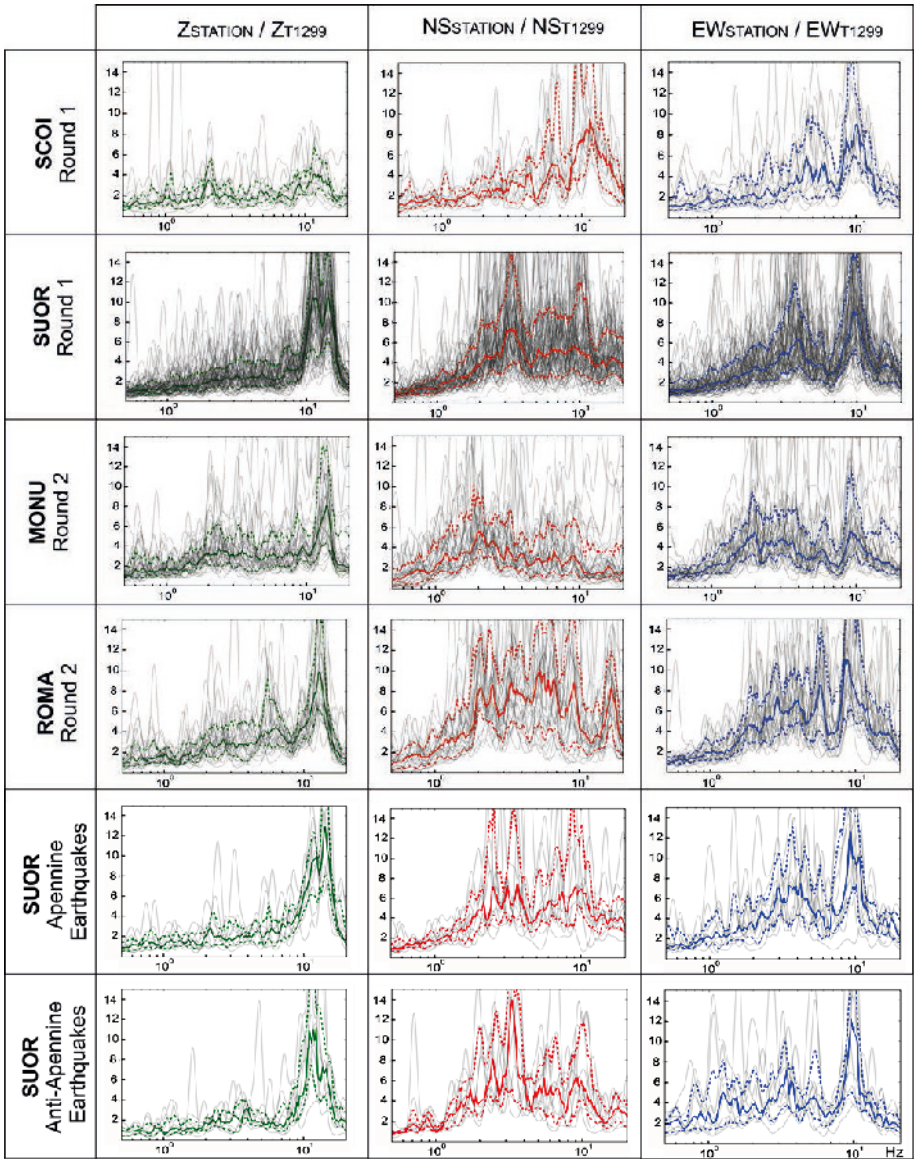

Fig. 4 Spectral ratios from SSR analyses on aftershocks: median curve (solid colour lines); 84th and 16th percentile curves (up and down dashed colour lines respectively). Note that the two sets of events (Apennine and Anti-Apennine site-source azimuth) were considered for the SUOR station

on the SSR curves for both the horizontal components; the greatest amplification peak is observed for the EW component at a frequency of about 10 Hz.

The SCOI station, located in the valley south of Amatrice hill opposite the T1299 reference station, shows a similar shape of the SSR curves for both the horizontal components, in contrast to all the other hill top stations. The most significant amplification values are concentrated at high frequencies, around 8–10 Hz (as for the vertical component), for both NS and WE components, and are lower than those calculated for the SUOR and ROMA stations.

HVSR analyses (Fig. 5) were first performed on the same time-windows of signals selected for the SSR analyses. Each spectral horizontal amplitude was computed as the geometric average of the corresponding spectral amplitudes of the two horizontal components; then, the horizontal to vertical spectral ratio (HVSR) was calculated. The HVSR curves resulting from these analyses are similar in shape to the SSR curves obtained for each station, especially if low frequencies are considered. As expected, the HVSRs for the T1299 reference station show approximately flat spectral trends for both noise and earthquake data sets (graphs in bottom row in Fig. 7).

In addition, HVSR analyses were performed on time windows for all the events acquired by each station and on noise time windows. Six 10-minute-long time windows of noise were manually selected, avoiding disturbances or transients. In this case, the HVSRs were computed as average estimates over 20.48-sec-long time-sub-windows. The results substantially confirmed

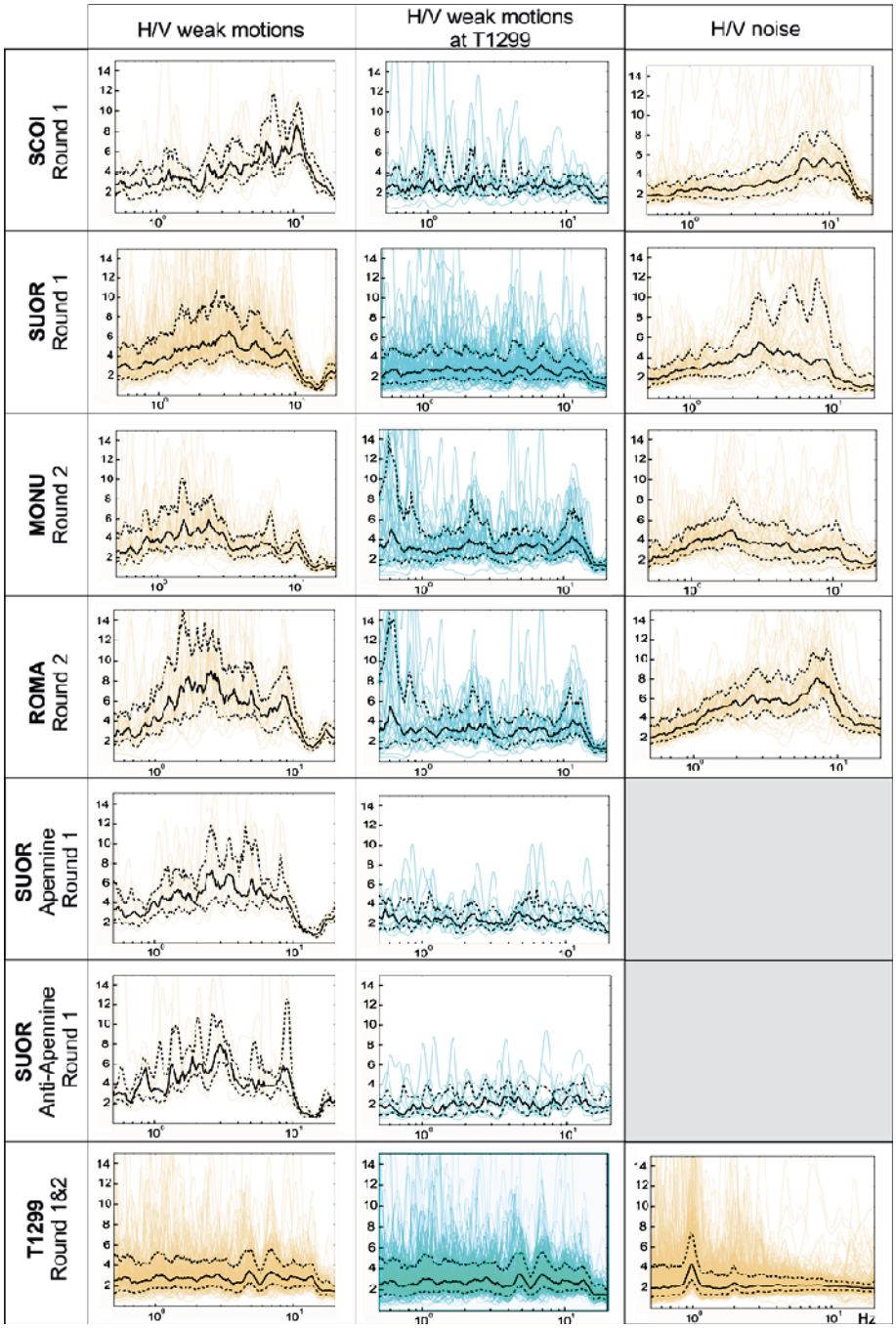

Fig. 5 Spectral ratios from the HVSR analyses (median curve in solid black line; 84th and 16th percentile curves in dashed black line). Left column: HVSR on weak motions for each seismic station; middle column: HVSR for T1299 station on the same weak motion sets as in the left column; right column: HVSR on noise for each seismic station (grey boxes are not covered by analyses)

the spectral trend obtained by applying the SSR analysis. Some differences are observed in both weak motion and noise HVSR curves for the T1299 and ROMA sites. At the ROME site, HVSRs amplification estimated from the earthquakes is higher than those estimated from noise at high frequencies, and vice versa at low frequencies. At T1299, the HVSR curves from weak motion show a narrow peak at 1 Hz (in a general flat trend) that did not appear in the noise HVSR curves.

3.3 Spectral directional analysis on weak motions and noise

The different spectral shapes resulting from the SSR analyses on the two horizontal components suggest a directional attitude of the seismic amplification at the hill-top sites. Therefore, directional spectral ratio analyses on the two horizontal projections of the particle ground motion were performed. The computation approach

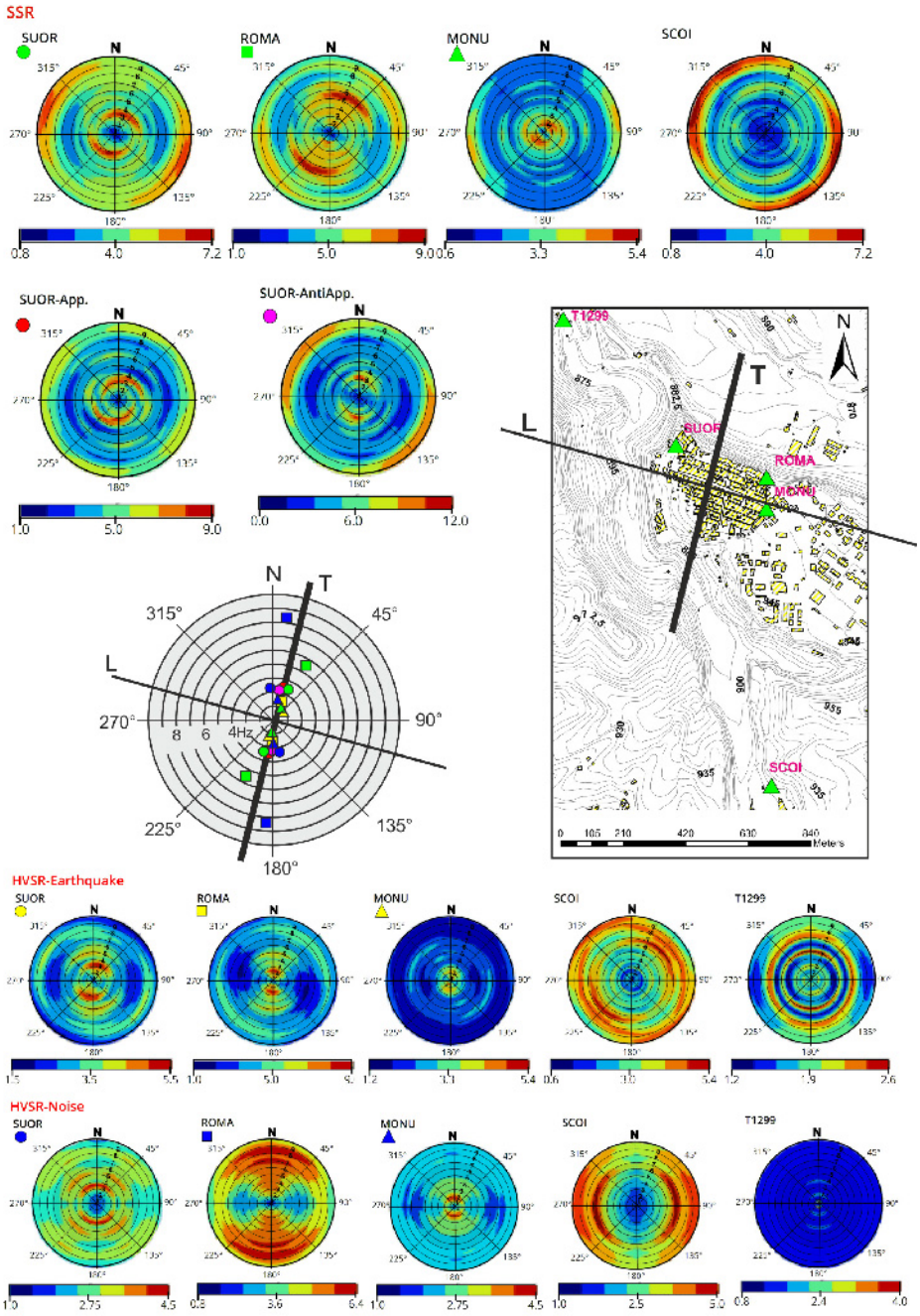

Fig. 6 SSR, HVSR-weak motion and HVSR-noise directional spectral analyses for the signals summarized in Table 1. Maximum values with respect to the transversal (T) and longitudinal (L) axes of Amatrice hill are represented in the central biggest polar diagram (symbols as reported on the top-left of small diagrams). Transversal and longitudinal axes of Amatrice hill and the seismic station sites are sketched in the map. The frequency step on the radial axis of the polar plots is 1 Hz

defines the wave field in the *x*-*y* projection plane, by rotating the components of ground velocity that are synchronously detected on the NS and EW directions. The directional spectral functions are defined in terms of median values at steps of 10°, and are plotted by using color map polar diagrams obtained by data interpolation (Fig. 6).

The results at the hill sites (SUOR, ROMA, MONU) show directional amplification in agreement with the hilly promontory orientation, which has longitudinal and transverse axes aligned, respectively, with N115E and N15E directions, in agreement with the Apennine chain axis. In contrast, a clear directional amplification does not appear at the valley site SCOI.

At the SUOR site, a double directional amplification effect can be observed. In fact, the amplification reaches maximum values both at a high frequency (9–10 Hz) in the N120E direction, and at a low frequency (3–3.5 Hz) in the N15E direction, in accordance with the longitudinal or transversal axes of Amatrice hill, respectively. When

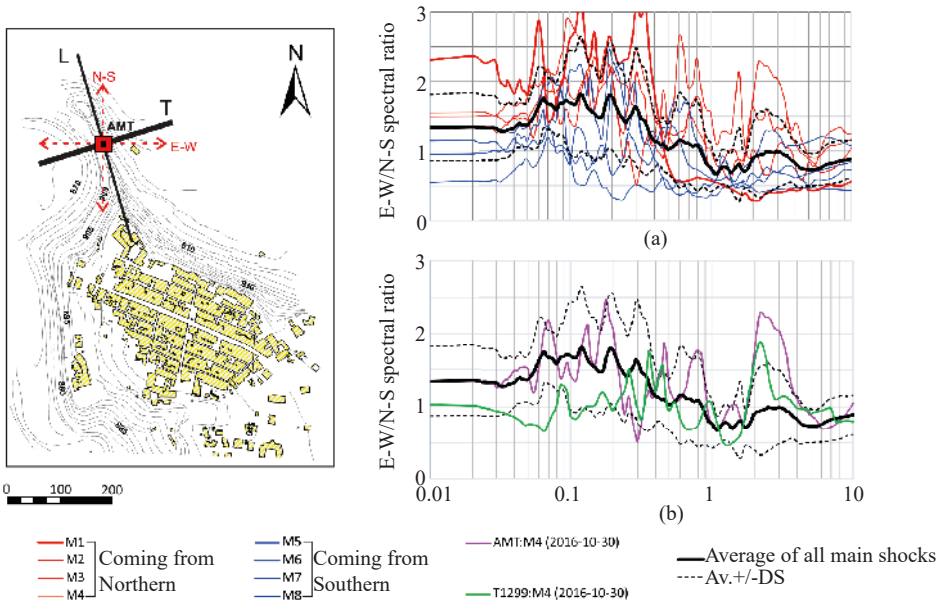

Fig. 7 Location of AMT station (left) and experimental topographic aggravation factor (TAF) results: a) EW/NS acceleration response spectral ratio (5% of critical damping) of strong motion events recorded at the AMT station; b) comparison between median TAF from M1 to M8 events and from the 2016-10-30 event at the AMT (magenta line) and T1299 (green line) stations

the Apennine and anti-Apennine clusters of events recorded by the SUOR station are separately anaylzed, amplification at low frequencies for both the two clusters of events can be observed; on the contrary, at high frequencies, marked amplification is recognized only for events with an anti-Apennine site-source azimuth (transversal hill axis). The anti-Apennine cluster analysis at the SUOR site provides the greatest amplification (up to 12) achieved among all the anaylzed sites, at low frequencies (3–3.5 Hz). At the ROMA site, the directivity analysis shows a substantial univocal azimuthal trend with significant amplification values in the 2–7 Hz frequency range. In that range, a sharper amplitude peak, around 4.5–6.0 Hz, was observed, approximately in the transversal direction of the hill. Finally, the MONU station shows a directional amplification in agreement with the transversal axis of the hill; however, the peak is located at a frequency (about 2 Hz) lower than those of the two other top-hill stations.

For the seismic stations at the top of Amatrice hill, the HVSR analyses, performed on the weak motion seismic records, confirm that the seismic amplification is azimuthally dependent, with maximum values along the direction of approximately N15–20E, that is approximately the orientation of the hill transversal axes. However, compared to the amplification from the SSR analyses, the HVSR results show some main differences: i) HVSR curves do not show amplification at a high frequency (9–10 Hz) with the exception of SCOI according to SSR analysis; ii) peak values generally occur at lower frequencies; and iii) the azimuthal trend of the HVSR maxima shows direction closer to the NS axis (about N5–10E) than the SSRs. In contrast, the valley stations SCOI and T1299 show HVSR maximum values with a large incoherent distribution on the polar frequency diagram, in particular, T1299 highlights a low and isotropic amplification.

In general, the SCOI station does not show the same directional amplification from SSR and HVSR analyses. In particular, the latter shows an extended azimuthal polarity centered along the N45 direction at 6–7 Hz that is not revealed by SSR analysis. In contrast, both SSR and HVSR analyses show a large azimuthal directionality on N315 at 9–10 Hz approximately corresponding to the longitudinal direction of the far Amatrice hill. Finally, a dispersive azimuthal distribution results from the noise HVSR analyses, with maximum values along with the NS direction for the hill stations, and along with the EW direction for SCOI; in contrast, no amplification is associated with T1299.

3.4 Spectral directional analysis on strong motions at AMT

Topographic effects from strong ground-motion recordings at the AMT permanent station were also investigated with the aim to give preliminary results about the topographic effects on Amatrice hill. The AMT station is located near the Red Zone at the top of an elongated ridge that has a high length/width ratio (of about 6). Since the major topographic effects are mainly related to the component of seismic shaking on the transversal axes of the ridge and the latter are counter-clockwise rotated only about nine-degrees with respect to the EW direction, the major topographic effects at the AMT station are/were expected in the EW component

of the recordings. A typical transversal cross-section of the ridge has the shape of small regular relief with a height of approximately 40 m from the valley. From this framework, the amplification due to the topographic effects are expected at short vibration periods (Geli *et al*., 1988; Paolucci *et al*, 2002), mainly acting on the EW direction. Against this background, an experimental topographic aggravation factor (TAF), defined in terms of the ratio between the acceleration response spectra of the EW and NS components of the recorded signals, could be used as a further amplification factor to highlight topographic effects at the AMT station. The so defined topographic aggravation factor was calculated for the eight strongest events in the seismic sequence (M1 to M8) (Fig. 7(a)). The median of this distribution shows a maximum aggravation factor values of about 1.7, in the period range 0.06–0.2 s (16.7–5.0 Hz) with significant values (>1.4) up to 0.3 s, and an aggravation factor on PGA equal to 1.35. In the distribution, the 24th August event (M1) seems to be an exceptional event with a PGA-aggravation factor value greater than 2.0 and EW/NS spectral ratio values exceeding 3.0 at low vibration periods. Supporting this approach, the topographic effect using the transversal (EW) on longitudinal (NS) response spectral ratio of the ground motions recorded in AMT, this same ratio, regarding the M4 earthquake (M=6.5 of the 30th October 2016) recorded at T1299 station (Fig. 6(b)), does not show amplitude in the same period range as the AMT site. This latter observation is also in accordance with the spectral ratio average of the all strong motions recorded in AMT.

4 Discussion

The severe damage that occurred during the 2016-2017 Central Italy seismic sequence in the Red Zone of Amatrice village, which is located at the top of a hilly plateau, suggested that local site effects may have played a significant role. The results of geophysical surveys and experimental analyses carried out on weak motion and noise recordings from temporary (SUOR, ROMA, MONU and SCOI) and permanent (AMT and T1299) seismic stations provided significant information on the subsoil layer sequence, as well as about the role and the nature of the seismic site effects affecting the ground response at the Red Zone of Amatrice hill.

The joint interpretation of data from the geological survey, boreholes, and geophysical investigation allowed an almost uniform sequence to be identified in the entire Red Zone that was in agreement with other studies focused on a larger investigation area (Milana *et al*. 2019). Shear wave velocities, derived for the characteristic geo-lithological sequence, are consistent with the lithological features and ages of the geological units ascribable to the sequence. In this sequence, a particularly significant seismic impedance contrast was found between the cover of soft deposits having an intra-mountain genesis, and the older-harder marine deposits constituting the structure of the relief. A second significant impedance contrast was identified inside these last deposits between an upper member composed of weak and degraded silico-clastic rocks and a basal rock unit with the same geological nature. In the Red Zone, the depth of this last member is comparable or just below the height of the hill (40–60 m).

The experimental seismic response was estimated via standard (SSR) and horizontal to vertical (HVSR) spectral ratio techniques at three recording stations placed in accessible sites of the Red Zone (SUOR, ROMA, MONU), which were affected by severe damage, and at another station (SCOI) located in a valley site characterized by soft covered material. SSR analyses were performed on two data sets of moderate events ($2.5 \leq M_w \leq 4.0$) of the sequence that occurred from January to August 2017. T1299 station, which belongs to the Italian National Seismic Network, was assumed as the reference station. This station was installed following the August 2016 event in a valley site, entailing the exclusion of the mainshock of the 24th in its recording dataset. For this site, no significant amplification was detected in a wide range of frequencies (1–10 Hz), by using HVSR analyses performed on the two earthquake datasets.

The comparison between SSR and HVSR amplification curves is summarized in Fig. 8(a) for all four recording temporary stations. In the comparison, SSR spectral ratio was calculated with reference to the geometric average of the corresponding spectral amplitudes of the two horizontal components. They show major differences at the SUOR and ROMA sites located at the border ridge; on the contrary, at the MONU site, located in the central sector of the hill, differences are negligible both in terms of spectral distribution and amplitude. This trend is probably due to the geometry of the hill. The SUOR site station is on a subordinate dorsal relief characterized by a shorter base than the main Amatrice's relief, promoting so the amplification peak at a higher frequency, 3–4 Hz, with respect to the central hill sector where MONU station was sited, about 2 Hz. In contrast, the edge of the ROMA site seems to conserve the amplification of the central sector of the hill plateau MONU with an additional amplification following the local high changing of the slope degree. This condition induces the local- multiple reflections of the waves involving the amplification at higher frequencies with values about 6–7 Hz. At the SCOI site, in the valley, SSR and HVSR curves are similar for most of the explored spectral interval (1–8 Hz). In this site, both techniques highlight the amplification at high frequency (10–15 Hz) different from the sites at top hill stations; this amplification can be due to the local geological sequence setting due to the presence of the shallow slim backfill. In all cases, the amplification from weak earthquakes is greater than that involved by noise according to previous experimental studies, pointing out that the amplification

increases with the amplitude of the seismic signal as long as the induced shear strain remains in the soil linear behavior domain (Horike *et al*., 2001; Pilz *et al*., 2009). On the other hand, it is not clear if the HVSR technique applied to strong motion detects the topographic effect in an appropriate manner. Theoretical studies (Bouckovalas and Papadimitriou, 2005) highlight that parasitic high-frequency waves, due to multiple reflections, develop more significant amplification/de-amplification of the vertical component in sites where the slope inclination change. The same evidence, on experimental data, is showed in Barani *et al*., 2014, Stolte *et al*., 2017. The ratio between the average SSR and HVSR spectral values (Fig. 8(b)) shows that significant under-estimation anomalies in the HVSR curves occur around 3.5 Hz for all the stations on the hill top, and much more at 5.5 Hz at the ROMA site. On the contrary, a substantially flat shaped SSR/HVSR spectral ratio, close to unit value, was found at the valley site, SCOI, in the frequency range of 1-8 Hz. This highlights that HVSR and SSR results proved to be good at detecting the site effect at flat sites, but less capable in relation to complex topographic sites such as SUOR and ROMA.

Although site effects cannot be assessed only on the basis of experimental data analyses, some substantial clues in this direction can be recognized by using such analyses, for the study area. High amplification was detected for all the stations located at the top of the hill. For these sites, the amplification from SSR analyses shows a significant variation in the frequency distribution related to the different sectors of the relief. This is consistent with previous experimental studies (Wood and Cox, 2016; Grelle *et al*., 2018b; Grelle *et al*., 2016), and numerical simulation analyses developed on uniform hilly plateaus or steep slope areas (e.g. Bouchon and Barker, 1996; Paolucci *et al*., 2002). In particular, amplification at low frequency (around 2 Hz) was observed in the central sector of the plateau (MONU) and an increase of this amplification at higher frequencies (3–5 Hz) was noted along the near ridge zones of the slopes where a sharper change of the slope-angles occurs (ROMA and SUOR).

In addition, mainly from SSR and HVSR analyses carried out on seismic weak motion recordings, a clear directionality of the seismic amplification was observed in accordance with the elongated shape of the hill. Specifically, the ground motion is amplified in a preferential directional running to 5°–20° N for all the top stations in agreement with the transversal elongation of the hilly plateau. Furthermore, the HVSR maxima values are closer to north (5°–10°) than that SSR maxima values; this effect may be due to the fact that the vertical component Z is also partially involved by the amplification along the direction that is nearly transversal to the hill (about 20°). In contrast, for the valley station (SCOI), the directional amplification maxima values were not observed in accordance with the transversal hill direction, while an incoherent isotropic distribution of the low-relevant maxima values are observed for T1299. These polar results are in accordance with the absence of the topographic effect promoted by the Amatrice hill in these two valley sites.

Finally, the directional effect, shown by the hilly site stations, remains almost unchanged when considering the seismic events split into two different Appenine and Anti-Appenine azimuths. In addition, although the

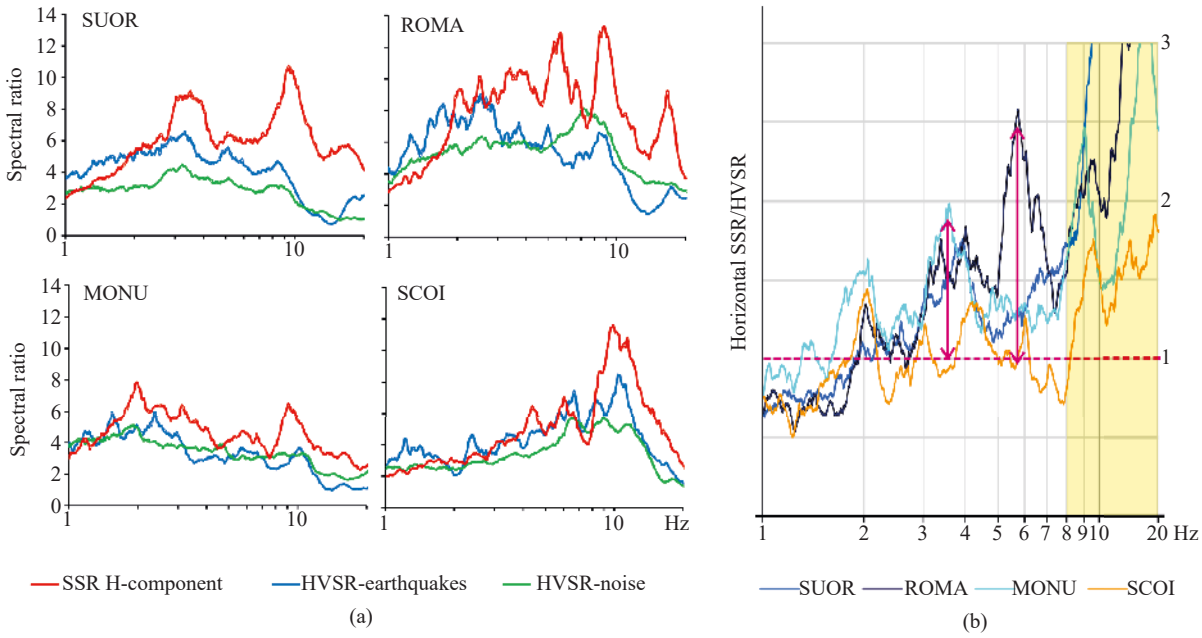

Fig. 8 a) Comparison between SSR and HVSR spectral ratios for all four seismic stations; b) ratio between SSR and HVSR analysis results for each station

directional effect on the seismic amplification seems to be confined to the ridge of the hill, the peak values progressively shift from higher frequency (4–6 Hz) at the edge of the slopes to lower frequencies (1.5–2.5 Hz) in the central zones of the hill.

5 Conclusions

The experimental study described herein supports the role of topographic effects in hilly zones. With regard to the Amatrice hill, these effects, which are manifested in the amplification of the ground motion, are mainly influenced by the plateau geometry of the relief and its orientation. On the hill, the spectral changes occur in relation to the position considered on it. From the results of two different observational methods, SSR and HVSR, it is possible to highlight some azimuthal differences of amplification peaks in the directional analysis considering some spectral intervals. This discordance is due to the fact that both the estimation models include different simplifications which are derived from assumptions that, in HVSR, the topographic effects do not influence the vertical component of the ground motions, and the site effects do not happen in the site of the reference station that was considered in SSR analysis. However, both have been used to better explain the phenomenology that occurred by reinforcing the reliability of the results where both converge. In addition, HVSR analysis was used to validate the choice of the reference station in SSR analysis, namely, when HVSR results have shown a flat spectral shape in agreement to the site morphology and geology.

The results highlight that the greater amplification occurs at the edge of the steep slope or where the zone is characterized by a greater three-dimensional change of the slope degree as in the dorsal zones. In general, the greatest amplification is mainly oriented transversally to the hill, in a range of 15°–25° NE, showing a spectral migration of the amplification peaks from 3–4 Hz at lower frequencies of around 2 Hz when passing from the edge of the hill zones at the central sector of the hilly plateau. In addition, other subordinate peaks of amplification detected at higher frequencies seems to be governed by local morphology of the surfaces that constitute the complex topographic zones of the relief.

Finally, the spatial trend and intensity, which are shown by observational spectral responses, are substantially in accordance with the numerical approach performed by some authors of this paper (Grelle *et al*., 2020) for the same zone of the Amatrice hill. In this paper, the authors have highlighted as the different spectral response computed at the top of the hill is also in agreement with the distribution of damage. More specifically, the results coming from the observational analysis can be used to give preliminary operational indications that can be used both in terms of reconstruction of the buildings and general seismic planning management.

Acknowledgement

This work benefits from reference elements and additional data from the Project “Interventi urgenti in favore delle popolazioni colpite dagli eventi sismici del 2016 (Urgent measures for the populations affected by the 2016 seismic sequence)”. The authors would like to thank the Italian Civil Protection Department (DPC) - Special Government Commissioner of the Presidency of the Council of Ministers - and the “Centro per la Microzonazione Sismica e le sue Applicazioni” which, respectively, have funded and coordinated the project. The authors are grateful to the National Order of Geologists for obtaining permission to access to the Red Zone of Amatrice as well as the DPC for granting it, and the firefighters for surveillance during the field survey. The suggestions of two anonymous reviewers helped improve the manuscript.

References

Ba Z, Liang J and Zhang Y (2017), “Diffraction of SH-Waves by Topographic Features in a Layered Transversely Isotropic Half-Space,” *Earthquake Engineering and Engineering Vibration*, **16**(1): 11–22.

Bakir BS, Sucuoglu H, Yilmaz T (2002), “An Overview of Local Site Effects and the Associated Building Damage in Adapazari during the 17 August 1999 İzmit Earthquake,” *Bull Seismol Soc Am*, **92**(1): 509–526. https://doi.org/10.1785/0120000819.

Barani S, Massa M, Lovati S and Spallarossa D (2014), “Effects of Surface Topography on Ground Shaking Prediction: Implications for Seismic Hazard Analysis and Recommendations for Seismic Design,” *Geophysical Journal International*, **197**: 1551–1565.

Boncio P, Lavecchia G, Milana G and Rozzi B (2004), “Seismogenesis in Central Apennines, Italy: An Integrated Analysis of Minor Earthquake Sequences and Structural Data in the Amatrice-Campotosto Area,” *Annals of Geophysics*, **47**(6): 1723–1742.

Bonnefoy-Claudet S, Baize S, Bonilla LF, Berge-Thierry C, Pasten C, Campos J, Volant P and Verugo R (2009), “Site Effect Evaluation in the Basin of Santiago de Chile Using Ambient Noise Measurements,” *Geophysical Journal International*, **176**: 925–937.

Borcherdt RD (1970), “Effects of Local Geology on Ground Motion Near San Francisco Bay,” *Bull Seismol Soc Am*, **60**: 29–61.

Bouchon M and Barker JS (1996), “Seismic Response of a Hill: the Example of Tarzana, California,” *Bull Seism. Soc. Am.*, **86**: 66–72.

Bouckovalas G and Papadimitriou A (2005), “Numerical Evaluation of Slope Topography Effects on Seismic Ground Motion,” *Soil Dynamics and Earthquake Engineering*, **25**: 547–558.

Buech F, Davies TR and Pettina JR (2010), “The Little

Red Hill Seismic Experimental Study:Topographic Effects on Ground Motion at a Bedrock-Dominated Mountain Edifice," *Bull. Seism. Soc. Am*., **100**(5A): 2219–2229.

Cara F, Di Giulio G, Milana G, Bordoni P, Haines J and Rovelli A (2010), "On the Stability and Reproducibility of the Horizontal-to-Vertical Spectral Ratios on Ambient Noise: Case Study of Cavola, Northern Italy," *Bull Seism Soc Am*, **100**(3): 1263–1275. doi: 10.1785/0120090086.

Cavinato GP and Celles PGD (1999), "Extensional Basins in the Tectonically Bimodal Central Apennines Fold-Thrust Belt, Italy: Response to Corner Flow Above a Subducting Slab in Retrograde Motion," *Geology*, 27, 955.

Cheloni D, De Novellis V, Albano M, Antonioli A, Anzidei M, Atzori S, Avallone A and Bignami C (2017) "Geodetic Model of the 2016 Central Italy Earthquake Sequence Inferred from InSAR and GPS Data," *Geophys. Res. Lett.*, **44**(13): 6778–6787, doi: 10.1002/2017GL073580.

Di Alessandro C, Bonilla LF, Boore DM, Rovelli A and Scotti O (2012), "Predominant-Period Site Classification for Response Spectra Prediction Equations in Italy," *Bull Seismol Soc Am*, **102**: 680–695. doi: 10.1785/0120110084.

Dolce M, Masi A, Marino M and Vona M (2003), "Earthquake Damage Scenarios of the Building Stock of Potenza (Southern Italy) Including Site Effects," *Bull Earthq Eng*, **1**: 115–140.

Facciorusso J, Madiai C and Vannucchi G (2016), "The 2012 Emilia Earthquake (Italy): Geotechnical Characterization and Ground Response Analyses of the Paleo-Reno River Levees," *Soil Dynamics and Earthquake Engineering*, **865**: 71–88. ISSN: 0267-7261, doi: 10.1016/j.soildyn.2016.04.017.

Gallipoli MR, Chiauzzi L, Stabile TA, Mucciarelli M, Masi A, Lizza C and Vignola L (2014), "The Role of Site Effects in the Comparison Between Code Provisions and the Near Field Strong Motion of the Emilia 2012 Earthquakes," *Bull Earthq Eng*, **12**: 2211–2230. http://dx.doi.org/10.1007/s10518-014-9628-7.

Gaudiosi I, Vignaroli G, Mancini M, Moscatelli M, Simionato M, Sirianni P, Razzano R, Peronace E, Piscitelli S, Madiai C and Amatrice Working Group (2019), "Site Effects in Saletta Damaged Area of Amatrice Municipality (Central Italy) After the 24th August 2016 Earthquake," *VII International Conference on Earthquake Geotechnical Engineering*, Rome, Italy, June 17-20.

Geli L, Bard PY and Jullien B (1988), "The Effect of Topography on Earthquake Ground Motion: A Review and New Results," *Bulletin of the Seismological Society of America*, **78**: 42–63.

Geological Map of Italy (1955), APAT, http://193.206.192.231/carta_geologica_italia/tavoletta.php?foglio=139

Grelle G, Bonito L, Lampasi A, Revellino P, Guerriero L, Sappa G and Guadagno FM (2016) "SiSeRHMap v1.0: A Simulator for Mapped Seismic Response Using a Hybrid Model," *Geoscientific Model Development*, **9** (4): 1567–1596.

Grelle G, Wood C, Bonito L, Sappa G, Revellino P, Rahimi S and Guadagno FM (2018b), "A Reliable Computerized Litho-Morphometric Model for Development of 3D Maps of Topographic Aggravation Factor (TAF): the Cases of East Mountain (Utah, USA) and Port au Prince (Haiti)," *Bulletin of Earthquake Engineering*, **16**(5): 1725–1750.

Grelle G, Bonito L, Maresca R, Maufroy E, Revellino P, Sappa G and Guadagno FM (2018a), "The Role of Topographic Effects on Amatrice′s Hill Detected by SiSeRHMap and Endorsed by Experimental Data and Damage Distribution," *16th European Conference on Earthquake Engineering*, Thessaloniki, Greece, June 18-21, extended abstract.

Grelle G, Gargini E, Facciorusso J, Maresca R and C Madiai (2020), "Seismic Site Effects in the Red Zone of Amatrice Hill Detected via the Mutual Sustainment of Experimental and Computational Approaches," *Bull Earthquake Eng*, **18**: 1955–1984. https://doi.org/10.1007/s10518-019-00777-z

Haghshenas E, Bard PY, Theodoulidis N and SESAME WP04 Team (2008), "Empirical Evaluation of Microtremor H/V Spectral Ratio," *Bull. Earthq. Eng*., **6**: 75–108. http://dx.doi.org/10.1007/s10518-007-9058-x

Hakima Djilali Berkane, Zamila Harichane, Erkan Çelebi and Sidi Mohammed Elachachi (2019), "Site Dependent and Spatially Varying Response Spectra," *Earthquake Engineering and Engineering Vibration*, **18**(3): 497–509. https://doi.org/10.1007/s11803-019-0517-6

Hartzell S, Meremonte M, Ramírez-Guzmán L and McNamara D (2014), "Ground Motion in the Presence of Complex Topography: Earthquake and Ambient Noise Sources," *Bulletin of the Seismological Society of America*, **104**(1): 451–466.

Horike M, Zhao B and Kawase H (2001), "Comparison of Site Response Characteristics Inferred from Microtremor and Earthquake Shear Waves," *Bull Seismol Soc Am*, **91**: 1526–36.

Hough SE, Altidor JR, Anglade D, Given D, Janvier MG, Maharrey JZ, Meremonte M, Mildor SL, Prepetit C and Yong A (2010), "Localized Damage Caused by Topographic Amplification During the 2010 M7.0 Haiti Earthquake," *Nat. Geosci*, **3**: 778–782.

Jahromi, SG and Karkhaneh S (2019), "The Plurality Effect of Topographical Irregularities on Site Seismic Response," *Earthquake Engineering and Engineering Vibration*, **18**(3): 521–534.

Kawase H (1996), "The Cause of the Damage Belt in Kobe: "The Basin-Edge Effect," Constructive Interference of the Direct S-Wave with the Basin-

Induced Diffracted/Rayleigh Waves," *Seismol. Res. Lett.*, **67**: 25–34. http://dx.doi.org/10.1785/gssrl.67.5.25.

Kawase H and Aki K (1990), "Topography Effect at the Critical SV-Wave Incidence: Possible Explanation of Damage Pattern by the Whittier Narrows, California, Earthquake of 1 October 1987," *Bull. Seismol. Soc. Am*., **80**(1): 1–22.

Konno K and Ohmachi T (1998), "Ground-Motion Characteristics Estimated from Spectral Ratio Between Horizontal and Vertical Components of Microtremor," *Bull. Seism. Soc. Am*., **88**: 228–241.

Lunedei E and Malischewsky P (2015), "A Review and Some New Issues on the Theory of the H/V Technique for Ambient Vibrations," In: Ansal A. (eds) Perspectives on European Earthquake Engineering and Seismology, *Geotechnical*, *Geological and Earthquake Engineering*, **39**: 371–394, Springer, Cham.

Madiai C, Facciorusso J and Gargini E (2017), "Numerical Modeling of Seismic Site Effects in a Shallow Alluvial Basin of the Northern Apennines (Italy)," *Bulletin of the Seismological Society of America*, **107**(5): 2094–2105. ISSN: 0037-1106, doi: 10.1785/01201602935.

Madiai C, Facciorusso J, Gargini E and Baglione M (2016), "1D Versus 2D Site Effects from Numerical Analyses on a Cross Section at Barberino di Mugello (Tuscany, Italy)," In: Procedia Engineering, *Procedia Engineer*, **158**: 499–504, Elsevier Ltd, ISSN: 1877–7058, Auditorium of Department of Arts of the Alma Mater Studiorum, ita, doi: 10.1016/j.proeng.2016.08.479.

Maresca R, Nardone L, Gizzi FT and Potenza MR (2018), "Ambient Noise HVSR Measurements in the Avellino Historical Center and Surrounding Area (Southern Italy), Correlation with Surface Geology and Damage Caused by the 1980 Irpinia-Basilicata Earthquake, *Measurement*, **130**: 211–222. doi: https://doi.org/10.1016/j.measurement.2018.08.015.

Maufroy E, Chaljub E, Theodoulidis NP, Roumelioti Z, Hollender F, Bard PY, De Martin F, Guyonnet-Benaize C and Margerin L (2017), "Source-Related Variability of Site Response in the Mygdonian Basin (Greece) from Accelerometric Recordings and 3D Numerical Simulations", *Bull Seismol Soc Am*, **107**(2): 787–808, DOI: 10.1785/0120160107.

Milana G, Cultrera G, Bordoni P, Bucci A, Cara F, Cogliano R, Di Giulio G, Di Naccio D, Famiani D, Fodarella A, Mercuri A, Pischiutta M, Pucillo S, Riccio G and Vassallo M (2019), "Local Site Effects Estimation at Amatrice (Central Italy) Through Seismological Methods," *Bull Earthq Eng*. https://doi.org/10.1007/s10518-019-00587-3.

Mucciarelli M and Gallipoli MR (2001), "A Critical Review of 10 Years of Nakamura Technique," *Boll. Geof. Teor. Appl.*, **42**: 255–256.

Mucciarelli M, Gallipoli MR and Arcieri M (2003), "The Stability of Horizontal-to-Vertical Spectral Ratio by Triggered Noise and Earthquake Recordings," *Bull Seism Soc Am*, **93**: 1407–1412.

Narayan JP and Singh SP (2006), "Effects of Soil Layering on the Characteristics of Basin-Edge Induced Surface Waves and Differential Ground Motion," *J Earthq Eng*, **10**(4): 595–614.

Pagliaroli A (2016), *Terremoto Italia Centrale del 24 agosto 2016: Valutazione Preliminare Degli Effetti di Sito*, Università di Chieti e Pescara "G. d'Annunzio, 14 ottobre 2016. DOI: 10.13140/RG.2.2.14134.09284.

Paolucci R (2002), "Amplification of Earthquake Ground Motion by Steep Topographic Irregularities," *Earthquake Engineering & Structural Dynamics*, **31**: 1831–1853.

Pauselli C, Barchi MR, Federico C, Magnani MB and Minelli G (2006), "The Crustal Structure of the Northern Apennines (Central Italy): An Insight by the Crop03 Seismic Line," *American Journal of Science*, **306**: 428–450.

Pergalani F, Pagliaroli A, Bourdeau C, Compagnoni M, Lenti L, Lualdi M, Madiai C, Martino S, Razzano R, Varone C and Verrubbi V (2019), "Seismic Microzoning Map: Approaches, Results and Applications After the 2016–2017 Central Italy Seismic Sequence," *Bull Earthq. Eng*., https://doi.org/10.1007/s10518-019-00640-1.

Pilz M, Parolai S, Leyton F, Campos J and Zschau J (2009), "A Comparison of Site Response Techniques Using Earthquake Data and Ambient Seismic Noise Analysis in the Large Urban Areas of Santiago de Chile," *Geophys J Int*, **178**: 713–728.

Rovelli A, Scognamiglio L, Marra F and Caserta A (2001), "Edge Diffracted 1-s Surface Waves Observed in a Small-Size Intramountain Basin," *B Seismol Soc Am*, **91**: 1851–1866.

Saeed Ghaff Arpour Jahromi and Sama Karkhaneh (2019), "The Plurality Effect of Topographical Irregularities on Site Seismic Response," *Earthquake Engineering and Engineering Vibration*, **18**(3): 521–534. https://doi.org/10.1007/s11803-019-0519-4

Sánchez-Sesma FJ, Perez-Rocha LE and Chávez-Pérez S (1989), "Diffraction of Elastic Waves by Three-Dimensional Surface Irregularities, Part II," *Bull Seismol Soc Am*, **79**: 101–12.

Sanchez-Sesma FJ, Rodriguez M, Iturraran-Viveros U, Rodrıguez-Castellanos A, Suarez M, Santoyo MA, Garcıa-Jerez A and Luzon F (2010), "Site Effects Assessment Using Seismic Noise," *Proceedings of the 9th International Workshop on Seismic Microzoning and Risk Reduction*, February 21–24, Cuernavaca, Mexico.

Sohrabi Bidar A, Kamalian M and Jafari MK (2009), "Time-Domain BEM for Three-Dimensional Site Response Analysis of Topographic Structures," *Int. Journal of Numerical Methods in Engineering*, **79**: 1467–1492.

Stolte AC, Cox BR and Lee RC (2017), "An Experimental Topographic Amplification Study at Los Alamos

National Laboratory Using Ambient Vibrations," *Bull. Seismol. Soc. Am.*, **107**: 1386–1401.

Wirth E, Marafi N and Stephenson W (2018), "Broadband Synthetic Seismograms for Magnitude 9 Earthquakes on the Cascadia Megathrust Based on 3D Simulations and Stochastic Synthetics, Part 1: Methodology and Overall Results," *B Seismol Soc Am*, **108**: 2347–2369. https://doi.org/10.1785/0120180034.

Wood CM and Cox BR (2016), "Comparison of Field Data Processing Methods for the Evaluation of Topographic Effects," *Earthquake Spectra*, **32**(4): 2127–2147.